



INVESTIGATING THE CORROSION AND MICROBIAL INHIBITING PROPERTIES OF SOME SULPHONAMIDE COMPOUNDS

*Adindu Chinonso Blessing^{1a}, Dike Kelechi Stanley^{2b}, Chidiebere Maduabuchi Arinzechukwu^{3c}, Ikpa Chinyere B. C.^{1d} and Okafor Kevin U.^{1e}

¹Department of Chemistry, Imo State University, P M B 2000 Owerri, Imo State Nigeria.

²Department of Microbiology, Imo State University, P M B 2000 Owerri, Imo State Nigeria.

³ Department of Science Laboratory Technology, Federal University of Technology, P.M.B. 1526 Owerri, Nigeria.

^ablessingojiegbe@yahoo.com,

^bkekedyke2000@yahoo.com,

^carinzechukwuchidiebere@gmail.com,

^dikpacbc@gmail.com, ^eugodolphine@gmail.com.

Corresponding author's phone number; 07030676855

Abstract

The corrosion and microbial growth-inhibiting properties of two sulphonamide compounds, 2-(phenylsulphonamido)-3-methylbutanoic acid (A) and 2-(4-Methylphenylsulphonamido)-3-methylbutanoic acid (B) were investigated. Gravimetric and electrochemical methods of corrosion study were used to keep the corrosion inhibiting process under surveillance in 1 M KOH. In contrast, the agar well diffusion technique was used to ascertain the biocidal activities of the compounds on four identified microbes; *Proteus mirabilis* MW016889, *Enterobacter hormaechei* MW016890, *Bacillus* sp MW016891 and *Thiobacillus* sp. The two compounds were found to simultaneously retard the corrosion process and microbial growth. The corrosion inhibiting properties may be attributed to the surface assimilation of the constituents on the corroding metal while the biocidal growth retardation is attributed to the disarray of the sprouting of the vital metabolic activities of the microbes. Quantum chemical computations and molecular dynamics simulations were used to ascertain the computational contributions of the compounds to the anti-corrosion activities. 2-(4-

Methylphenylsulphonamido)-3-methylbutanoic showed better inhibiting properties, and this may be attributed to its higher atomic mass.

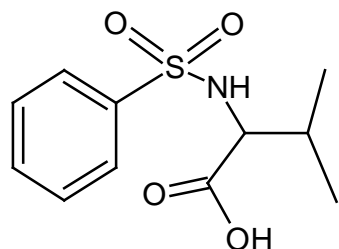
Keywords: corrosion; antibacterial; biocide; sulphonamide; and inhibition

1. Introduction

Metallic corrosion has been a cause of worry to manufacturers in recent decades. All structural metals corrode to some extent in chemical environments. Despite many corrosion prevention data available, the problem has persisted. Draconian environmental effects have deficient the use of inorganic materials for corrosion control. Such materials which include chromates, oxides nitriles etc. are being replaced with innocuous organic materials.^{1,2} These substances are known to adsorb on the surface of the metallic material, thereby obstructing the action centre on the metal facet, hence retarding the metal corrosion.

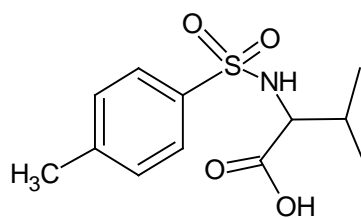
Sulphonamide compounds have been reported to inhibit the multiplication of pathogenic (substances that cause illness) microorganisms and form the significant agent in the synthesis of some useful pharmaceutical drugs.^{3,4} Attempt to supplement the field of application of these sulphonamide compounds to material protection in aqueous environments is gaining interest in the research industry.⁵⁻⁷ An essential supposition in our present finding is that the reported antibacterial effects of these synthetic materials could be extrapolated to reducing the crucial metabolic activities of corrosion-related microorganisms.⁸⁻¹⁰ These materials may also be thought to reduce microbial induced corrosion.

This report seeks to extend the field of application of sulphonamide compounds to material protection and investigate the inhibitive effects of the compounds on the corrosion of mild steel in 1 M KOH and also the biocidal activities of the compounds on the corrosion associated microorganisms.⁷ weight loss, Potentiodynamic polarization and electrochemical impedance spectroscopy methods of monitoring corrosion were used for the corrosion study while scanning electron ,microscopy was used to examine the metal microstructure. To computationally evaluate the distinctive input of the synthetic sulphonamide compounds, to the inhibition experience, some density functional theory (DFT) based quantum chemical calculations were exploited. The agar well diffusion method was used for the antibacterial analysis to ascertain the growth retardation ability of the sulphonamide materials on the identified microbes.



2-(Phenylsulphonamido)
-3-methylbutanoic acid

(A)



2-(4-Methylphenylsulphonamido)
-3-methylbutanoic acid

(B)

Figure 1 molecular formulae of the sulphonamide compounds

2. Materials and Experimental Section

2.1. Preparation of Materials

2.1.1. Inhibitor Preparation

The sulphonamide compounds used in this project were synthesized in the organic chemistry laboratory of the Imo State University Owerri.^{11, 12} 5g of each sulphonamide compound was dissolved in 1 L of distilled water to obtain 5 g/L solution which was subsequently diluted to the desired concentrations 0.2 mg/L, 0.4 mg/L, 0.6 mg/L, 0.8 mg/L and 1.0 mg/L.

2.1.2. Metal Preparation

The percentage composition by mass of the metal specimen utilized in the weight loss experiment is C – 0.05; Mn – 0.6; P - 0.36; Si – 0.3 and Fe-98.69 with a dimension of 3 cm × 3 cm × 0.14 cm, purchased from a commercial metal dealer in Owerri Imo State. The metal surfaces were scraped away under flowing water with silicon carbide abrasive paper,^{13, 14} of strength #400-#800, rinse in clean water, cleaned with acetone to dryness, weighed and preserved in a dry desiccator for use when desired.¹⁵ For the electrochemical tests, mild steel of dimension 1 cm × 1 cm 0.14 cm were used. The metals were encased in polytetrafluoroethylene (PTFE) rods with the aid of epoxy resin,^{16,17} leaving only a part (1 cm²) of the metal uncovered, and the denuded part was prepared as described above.

2.1.3. Solvents Preparation

All media distilled water used for this project was autoclaved at 121 °C for 15 minutes. 1 M KOH was used as the corrodent and was prepared from a high-quality analytical reagent.

2.2. Experimentals

2.2.1. Isolation of Microorganisms

Scrapings from corroding pipeline were obtained from the equipment of Total oil and gas company along Okigwe road Owerri. Samples were aseptically collected in sterile polythene bags and transported in a cold box containing ice to microbiology laboratory of Imo State University Owerri. Serial dilutions obtained from the scrapings were achieved and utilized for isolation of aerobic bacteria on Nutrient agar and sulfate-reducing bacteria on Winokrasky medium. The spread plate technique was employed for inoculation. Nutrient agar plates were incubated at 37⁰C for 24h while Winokrasky agar plates were incubated anaerobically at 35⁰C for 48h.

2.2.2. Identification of Microorganism

Isolates were preliminarily identified to genus level based on their morphological (cellular shape and arrangement, Gram reaction) and biochemical characteristics (catalase, oxidase, indole, urease). Based on their preliminary result, four isolates preserved in tryptone soy broth were sent to Inquaba biotech South Africa for sequencing.

2.2.3. Molecular Characterization

Extraction of genomic DNA was performed with ZR Soil Microbe DNA miniprep extraction kit (Zymo Research Corporation, Irvine, CA, USA) without modifications. The integrity of DNA was done using 1% agarose gel electrophoresis and quantified using Nanodrop spectrophotometer (3300).

2.2.4. 16S rRNA Sequencing Method

16S rRNA gene PCR amplification and sequencing were done by Inquaba Biotech, a commercial service provider located in South Africa. The primers 27F and 1492R were used, PCR reaction was performed with 20nm of genomic DNA as the template in a 30µl reaction mixture by using OneTaq Quick-load 2X Master Mix (Biolab, USA). Amplified PCR product was sequenced using ABI Prism 3730xlDNA analyzer (Applied Biosystems, Foster City, CA).

2.2.5. Phylogenetic Analysis

DNA sequencing analysis was done following standard procedures. Contiguous sequence reads were obtained using Bioedit software package and subsequently aligned using CLUSTAL (version 1.2.4). The 16rRNA sequences of bacteria obtained from this study were compared with sequences in the GenBank using the Basic Local Alignment Search Tool,¹⁸ for nucleotide sequences (*blastn*)

2.2.6. Gravimetric Experiment

The gravimetric tests were achieved by metal submersion method in a 300 ml of the test solution perpetuated at 300 K. The earlier prepared mild steel coupons were hanged from support into containers of the system.¹⁹ To ascertain the reduced weight after a given time, the mild steel coupons were removed, soaked in a solution having 20 % NaOH and 200 g/L zinc dust to quench corrosion, washed with distilled water while scrubbing with a bristle brush, dried using acetone, weighed and re-inserted into the test container.²⁰ This was done at 24 h interval ceaselessly for a period of 120 h. The weight loss at a particular hour was calculated by subtracting the weight at a given time from the earliest weight of the metal.²¹ The average of triplicate measurements was calculated to give the gravimetric data.

2.2.7. Electrochemistry Experiment

A standard three-electrode glass 400 mL cell was utilized in a VERSASTAT 400 Complete DC Voltammetry and Corrosion System installed with a V³ Studio software.²² The metal coupon dipped in a 1M KOH electrolyte was the working electrode as graphite, and saturated calomel electrode (SCE) was the counter and reference electrodes used for the electrochemical study. The saturated calomel electrode was joined to the cell using a Luggin's capillary.²³ Impedance data were obtained at corrosion potentials (E_{corr}) using a range of frequency of 100 kHz–10 MHz,²⁴ at perturbation amplitude of 5 mV, the potential capacity for the potentiodynamic polarization experiment was ± 250 mV versus corrosion potential at 0.333 mV/s scan rate.²⁵ The experiments were conducted three times, and the average values serve as the electrochemistry data.

2.2.8 Scanning Electron Microscopy examination (SEM)

Surface morphology of the mild steel metal was studied using scanning electron microscopy Shimadzu SSX-550. Metal coupons of 15 × 10 × 2 mm were polished and prepared as in the gravimetric experiment, immersed for 24-h in the KOH solution without and with the sulphonamide inhibitors at 30 °C, washed in distilled water, dried in acetone and submitted for SEM analysis.

2.2.9 Antibacterial Experiment

The agar well diffusion method was used for the antibacterial experiment.²⁶ Pure cultures of each isolate were grown on Nutrient broth for 18 h at 37°C. The concentration of each inoculum was adjusted with sterile normal saline to the turbidity of 1.5×10^8 CFU/ml (0.5McFarland standard). 0.1ml was inoculated unto sterile Muller Hilton agar by spreading. A sterile cup borer was used to create wells (15 mm) in the inoculated plate. Synthesized compounds were aseptically added into the wells using a 2ml micropipette. The plates were kept on

the laboratory bench to allow the synthesized compound to diffuse into the agar and subsequently incubated at 37°C.

2.2.10 Identification of Bacteria

A total of four bacteria genera comprising *Proteus mirabilis* MW016889, *Enterobacter hormaechei* MW016890, *Bacillus* sp MW016891 and *Thiobacillus* sp were identified. Mesophiles such as *Proteus* and *Bacillus* have previously been isolated from corroded metal material.²⁷ The Sulphur reducing bacteria thiobacillus has been implicated repeatedly from several studies.^{28,29}

3. Results and Discussion

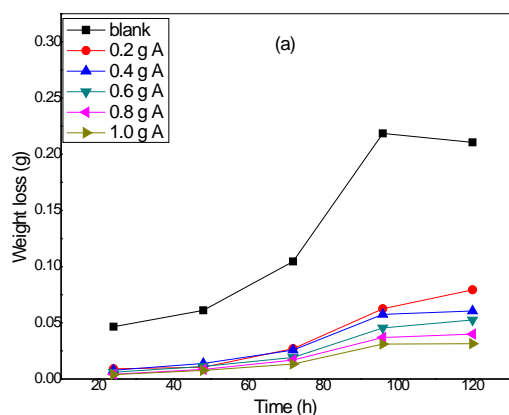
3.1. Gravimetric Result

Gravimetric tests were performed on the mild steel coupons, and the results are presented in figures 2 and 3, respectively. From the results, it can be inferred that the sulphonamide compounds reduced the corrosion of mild steel to a reasonable extent as weight loss is seen to decrease with increase in the concentration of the inhibitor.

The efficacy of the compounds as inhibitors was evaluated as below;

$$IE_W\% = \left(1 - \frac{\Delta W_{inh}}{\Delta W_{blank}}\right) \times 100 \quad (1)$$

Where W_{inh} and W_{blank} represent weight reduction in the inhibited and uninhibited systems.



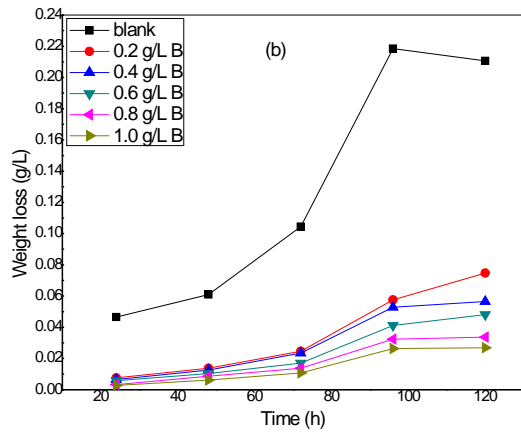


Figure 2 Graph of weight loss vs time for mild steel corrosion for compounds A and B respectively

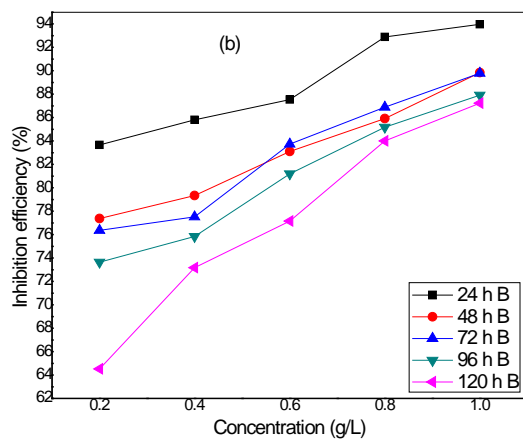
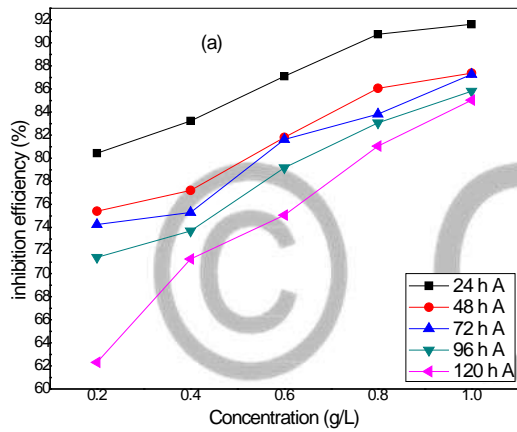


Figure 3 Graph of inhibition efficiency vs concentration for mild steel corrosion for Compounds A and B respectively

3.2 Electrochemistry Results

3.2.1. Potentiodynamic Polarization Results

Polarization experiments were conducted to explore the influence of the sulphonamide additives on the anodic and cathodic half-reactions of the electrochemical process. Mild steel Potentiodynamic polarization (PDP) behaviour in 1 M KOH in the absence and present of the sulphonamide additives are shown in figures 4 and 5 while the PDP parameters comprising corrosion current density values (I_{CORR}), the corrosion potential (E_{CORR}) and the effectiveness of the inhibition **IE** % calculated from the exploration of the polarization curves are shown in Tables 1&2 for compounds A and B respectively.

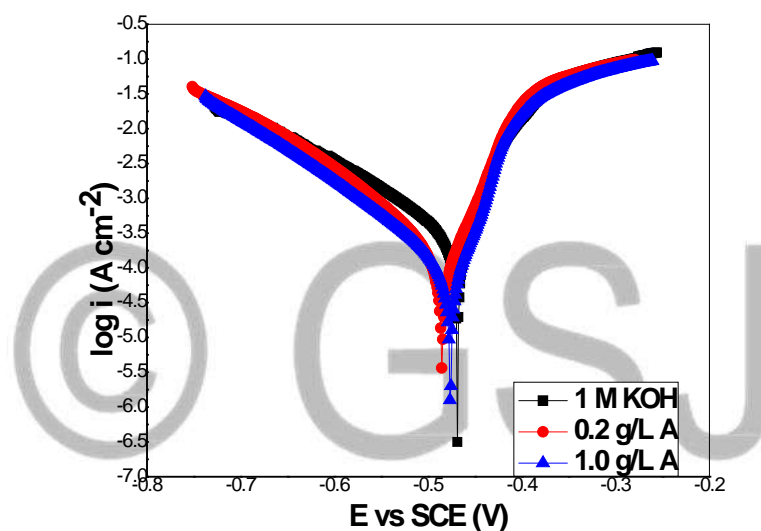


Figure 4: Potentiodynamic polarization curves of Mild steel in 1 M KOH in the absence and presence A.

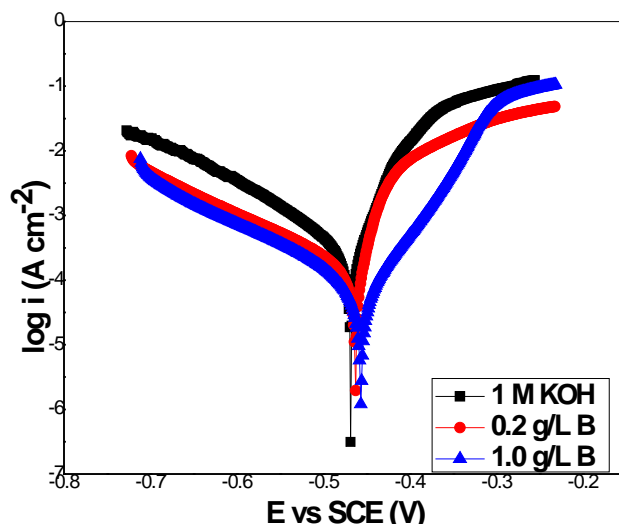


Figure 5: Potentiodynamic polarization curves of Mild steel in 1 M KOH in the absence and presence B.

The inhibition effectiveness (IE %) was evaluated from the values of the corrosion current densities without $I_{corr,bl}$ and with $I_{corr,inh}$ the presence of the sulphonamide additives according to the relationship below;

$$IE\% = \frac{I_{corr,bl} - I_{corr,inh}}{I_{corr,bl}} \times 100 \tag{2}$$

A critical examination of the polarization results in Figures 4 & 5 and Tables 1&2 shows that the presence of the sulphonamide inhibitors reduced significantly, the corrosion current densities (I_{corr}) from the values they had in the uninhibited system, the reduction is more pronounced with the increase in concentration. Also, the presence of the inhibitors affected significantly the cathodic and even the anodic half-reactions shifting the corrosion potential (E_{corr}) slightly towards the negative (cathodic) half-reaction in A and somewhat towards the positive (anodic) half-reaction in B.

Table 1. Electrochemical Parameters for Mild in corrosion 1 M KOH in the Absence and Presence of A.

System	E_{corr} (mV vs SCE)	I_{corr} ($\mu A/cm^2$)	IE %	R_{ct} (Ωcm^2)	$Q_{dl}(\mu\Omega^{-1} S^n cm^{-2})$ $\times 10^{-4}$	n	IE %
1M KOH	-463	210.3		155.2	71.5	0.88	

0.2 g/L A	-483	69.7	66.9	349.7	30.2	0.88	55.6
1.0 g/L A	-494	40.3	80.8	494.6	20.5	0.89	68.6

3.2.2. Impedance Results

Impedance experiments were accomplished to understudy the kinetics of the electrochemical processes and also to gain insight into the mechanism of the Fe/KOH edge with or without the sulphonamide inhibitors. The Nyquist formats of the impedance responses are given in Figures 6 and 7 also; the impedance parameters are shown in Tables 1&2. The Nyquist plots show only one hollow half-circle in the high-frequency region.³⁰ The depression that is observed in the Nyquist plots centred under the real axis is typical of most solid metallic materials having frequency dispersion of the impedance details.³¹ A solution resistance (R_s) represents the transfer function, which is shorted by a capacitor C placed in parallel with the charge transfer resistance (R_{ct}) according to

$$Z_{\omega} = R_s + \left(\frac{1}{R_{ct}} + j\omega C \right)^{-1} \quad (3)$$

This transfer function can only be used when dealing with systems in the same physical phase hence cannot give the reason for the capacitive loop depression. For non-ideal frequency systems, however, a constant phase element (CPE) replaces the capacitor, and this gives the reason for the deviation from the ideal dielectric system. The CPC impedance is then given by

$$Z_{CPE} = Q_{dl}^{-1} (j\omega)^{-n} \quad (4)$$

Where Q_{dl} represents CPE constant and n is the CPE exponent while $j = (-1)^{1/2}$ represents an imaginary number and ω is the angular frequency measured in radian, and it is equal $2\pi f$ and $f =$ frequency in Hz. The Q_{dl} values were calculated from the R_{ct} values with the relationship.

$$Q_{dl} = \frac{1}{2\pi R_{ct} f} \quad (5)$$

The impedance spectra were accordingly fitted into an equivalent circuit $R_s(Q_{dl}R_{ct})$ to obtain the impedance parameters.³² The electrochemical data in Tables 1 and 2 show that the magnitude of the R_{ct} increased when the inhibitor is introduced and then increased further with concentration with a corresponding decrease in the value of Q_{dl} which is the reason for the increase in the size of the capacitive semicircle showing that the inhibitor is

effective for the systems studied. The reduction in the Q_{dl} values as the inhibitor concentration increased which usually occur when the dielectric constant reduces or as the double layer solidness increases may be due to the adsorption of the sulphonamide compounds (having smaller dielectric constant when compared to the adsorbed water molecules that they displaced) on the mild steel/ inhibitor surface and hence protecting the metallic material from corrosion.

The values of IE % for the impedance experiments were obtained by comparing the value of R_{ct} with and without the inhibitor as follows;

$$IE(\%) = \left(\frac{R_{ct,inh} - R_{ct,bl}}{R_{ct,inh}} \right) \times 100 \quad (6)$$

Where $R_{ct,inh}$ is the R_{ct} value when the inhibitor was added and $R_{ct,bl}$ is the R_{ct} value in the blank solution.

Table 2. Electrochemical Parameters for Mild steel in 1 M KOH in the Absence and Presence of B.

System	E_{corr} (mV vs SCE)	I_{corr} ($\mu A/cm^2$)	IE %	R_{ct} (Ωcm^2)	$Q_{dl}(\mu\Omega^{-1} S^n cm^{-2})$ $\times 10^{-4}$	n	IE %
1M KOH	-463	210.3		155.2	71.5	0.88	
0.2 g/L B	-456	38.9	81.5	640.9	17.2	0.87	75.8
1.0 g/L B	-449	25.8	87.7	892.5	12.5	0.89	82.6

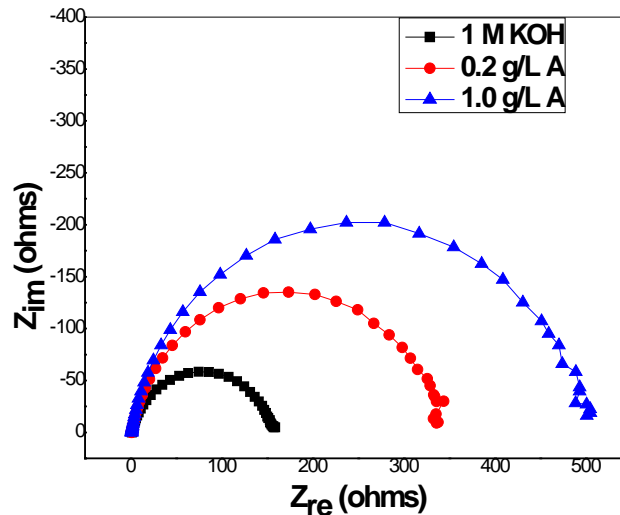


Figure 6. Electrochemical impedance spectroscopy for Mild steel in 1 M KOH in the absence and presence of A.

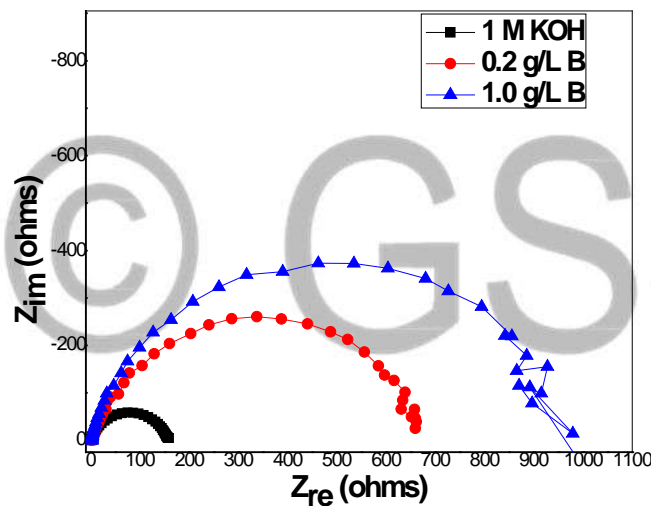


Figure 7. Electrochemical impedance spectroscopy for Mild steel in 1 M KOH in the absence and presence of B.

3.2. Scanning Electron Microscopy (SEM) Results

Surface characteristic of the metal before and after immersion of the mild steel in the aggressive solution without and with the inhibitors was done using scanning electron microscopy. Figure 8 shows the SEM images of the mild steel coupons before immersion in the aggressive solution (a), after immersion in 1 M KOH (b), and after immersion in the aggressive solution with in the presence of A (c) and in B represented in 8 c. The image in

Figure 8 shows that the mild steel coupons were severely damaged when exposed to the aggressive solution without the sulphonamide inhibitor (Figure 8 b) compared to when the inhibitors were added (Figures 8c and 8d).

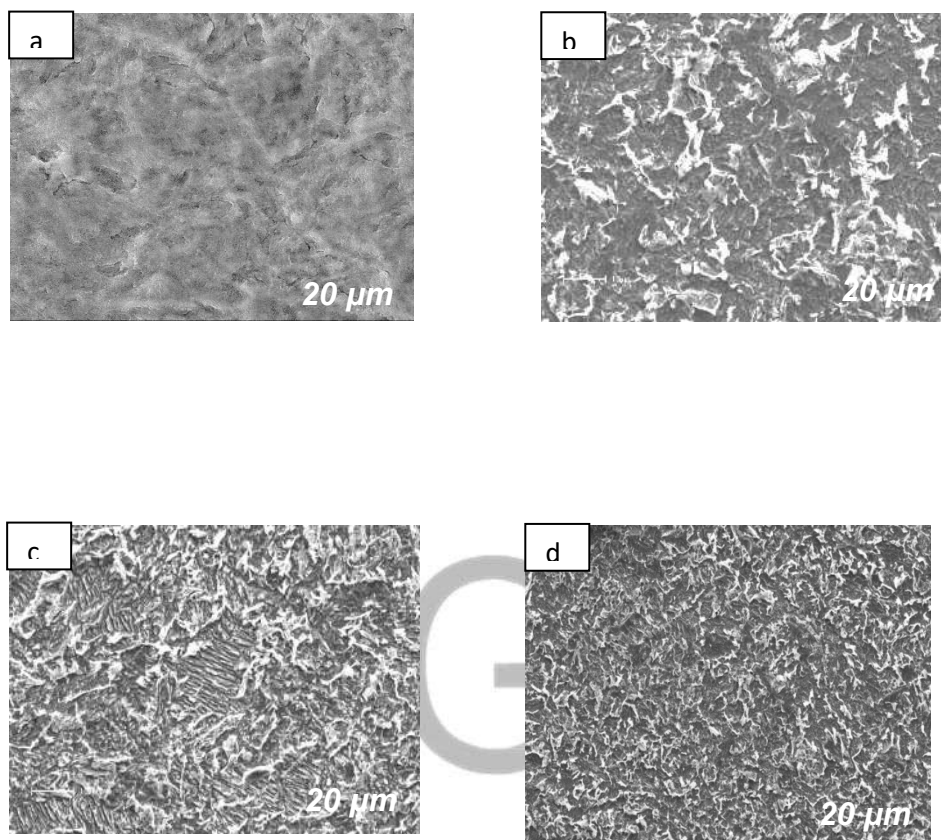


Figure 8, SEM images of the metal before immersion (a), after immersion in the blank 1 M KOH solution (b), in 1 M KOH+A (c) and in 1 M KOH+B (d)

3.3. Antibacterial Result

The result shows that the inhibitory effect of compound A increased as the concentration increased. The highest inhibition was recorded against *Proteus mirabilis* (15 mm) and *Bacillus* sp (12mm). For compound B, inhibitory activity was more pronounced against *Enterobacter hormaechei* and *Thiobacillus* sp. The inhibitory result is shown in Tables 3 and 4, respectively.

Table 3 Antibacterial Result for A

Concentration (g/L)	Zone of Inhibition (mm) for the organisms			
	<i>Enterobacter hormaechei</i> MW016890	<i>Thiobacillus</i> sp	<i>Proteus mirabilis</i> MW016889	<i>Bacillus</i> sp MW016891
0.2	4	5	6	4
0.4	6	6	8	6
0.6	8	10	10	8
0.8	10	8	11	10
1.0	11	10	15	12

Table 4 Antibacterial Result for B

Concentration (g/L)	Zone of Inhibition (mm) for the organisms			
	<i>Enterobacter hormaechei</i> MW016890	<i>Thiobacillus</i> sp	<i>Proteus mirabilis</i> MW016889	<i>Bacillus</i> sp MW016891
0.2	8	8	4	2
0.4	10	9	6	4
0.6	11	11	7	7
0.8	12	14	9	8
1.0	14	16	11	9

3.4. Computational Result

Already, experimental data has shown that the inhibitive effect of the chosen sulphonamide compounds may be ascribed to the surface assimilation of the constituents on the surface of the mild steel. Further evidence of the surface assimilation is obtained from quantum chemical computations and molecular dynamics modeling, such calculations were achieved to highlight the arrangement of atoms in the compounds thus establishing the reaction site and also the local reactivity of the compound. Our data computation was made possible using Density functional theory (DFT) electronic structure program DMol³ with a Mulliken population analysis.³³ The electronic data for the said modeling is the Perdew–Wang (PW) local correlation density functional as well as the restricted spin polarization using the DND basis set. COMPASS force field and the Smart minimize method using high-convergence criteria were employed for geometry optimization.

The electronic structure of the molecule was then modeled, this to indicate the apportioning of the frontier orbitals, to show the reaction emplacement and the local reactivity of the molecules. The optimized structures, highest occupied molecular orbital (HOMO), lowest unoccupied molecular orbital (LUMO), and also the electron densities of the molecules are shown in Figure 9 while Table 5 shows the corresponding computed quantum chemical parameters for the most stable arrangement of the molecules which include Homo energy (E_{HOMO}), Lumo energy (E_{LUMO}), Energy gap ($E_{\text{LUMO}-\text{HOMO}}$), absolute electronegativity (X), absolute hardness (η), electron charge transfer (ΔN), absolute softness (σ) and the adsorption energy. The result showed that the values correspond with that already reported for some organic compounds.³⁴ Interestingly, high-value Homo energy (E_{HOMO}) reflects a higher tendency of the compound to give an electron to the unoccupied d-orbital of the mild steel. Similarly, the low value of the energy gap ($E_{\text{LUMO}-\text{HOMO}}$) shows that the energy needed to detach an electron from the least occupied orbital is likely to be low giving rise to in high inhibiting power. The Homo and Lumo energies are related to the ionization potential (I) and electron affinity (A) as below,³³

$$I = -E_{\text{HOMO}} \quad (7)$$

$$A = -E_{\text{LUMO}} \quad (8)$$

Electron transfer (ΔN) from the inhibitor which functions as a Lewis base to the metal which functions as a Lewis acid is calculated with the equation below;

$$\Delta N = \frac{\chi_m - \chi_i}{2(\eta_m + \eta_i)} \quad (9)$$

Where χ_m and χ_i represent the absolute electronegativity of the mild steel and the sulphonamide compound respectively; while η_m and η_i stand for their corresponding absolute hardness. The theoretical values of 7 eV/mol and 0 eV/mol for χ_m and η_m where used to calculate the values of ΔN presented in Table 5. ΔN values have been shown to relate well with adsorption energy with the high value showing stronger adsorption of the sulphonamide compound to the mild steel surface. The relationship between χ , η , A and I are given below;

$$\chi = \frac{I+A}{2} \quad (10)$$

$$\eta = \frac{I-A}{2} \quad (11)$$

The chemical hardness/softness has been reported to be a significant indicator of the tendency of the molecules towards molecular interaction hence softness encourages close attachment between the inhibitor and metal surface and also blending with the metal state.³⁴ Equation 12 shows the relationship between absolute hardness and softness.

The reactivity order of the sulphonamide compound is 2-(4-methylphenylsulphonamido)-3-methylbutanoic acid > 2-(phenylsulphonamido)-3-methylbutanoic acid as calculated from our quantum chemical computation.

$$\sigma = \frac{1}{\eta} \quad (12)$$

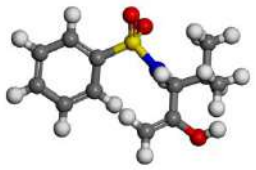
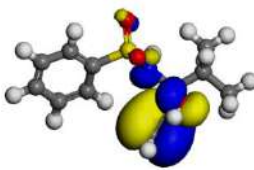
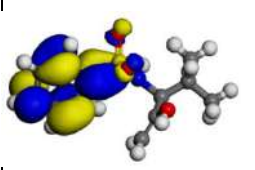
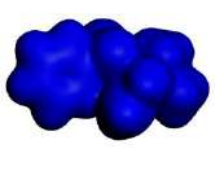
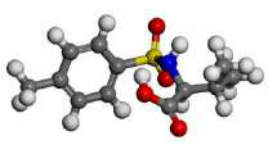
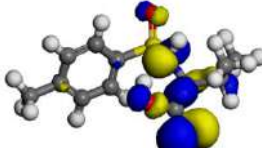
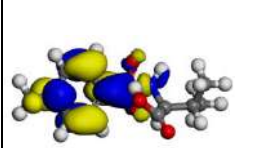
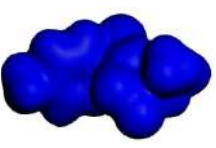
	Optimized structure	Homo orbital	Lumo orbital	Electron density
2-(phenylsulphonamido)-3-methylbutanoic acid (A)				
2-(4-methylphenylsulphonamido)-3-methylbutanoic acid (B)				

Figure 9 Electronic properties of the sulphonamide compounds

Table 5 Calculated quantum mechanical parameters for the sulphonamide compounds

Quantum chemical mproperty	2-(phenylsulphonamido)-3-methylbutanoic acid (A)	2-(4-methylphenylsulphonamido)-3-methylbutanoic acid (B)
E_{HOMO} (eV)	-5.491	-6.041
E_{LUMO} (eV)	-1.557	-2.181
$E_{\text{LUMO}} - E_{\text{HOMO}}$ (eV)	3.934	3.860
χ	3.524	4.111
η	1.967	1.930
ΔN	0.884	0.748
σ	0.508	0.518
Adsorption energy (kcal/mol)	-124.27	-133.17

3.5. Molecule dynamic simulations (MD)

Molecule dynamic simulations were used to analyze the surface assimilation of the sulphonamide compounds on the surface of the mild steel. Forcite quench molecular dynamics was used to analyze different low energy arrangements to pick out the small energy minima.³⁵⁻³⁷ COMPASS force field and the Smart algorithm were utilized in the calculations. The simulation box has the dimension $30 \text{ \AA} \times 25 \text{ \AA} \times 29 \text{ \AA}$ having periodic boundary conditions to simulate a part of the surface having no arbitrary boundary conditions.³⁸⁻⁴⁰ The box held the metal slab split alongside the Fe (110) flat surface. The height of the vacuum layer was 20 \AA . Prior to the optimization of the Fe (110) plane, the conformation of the down surface of the slab was impelled to the bulk of the positions and other degrees of freedom were eased. The metal surface was then extended into a 20×8

supercell. The adsorption of the compound was only on one side of the slab. The temperature of adsorption was 303 K with NVE (microcanonical) entity; the time step was 1fs and simulation time of 5ps. Quenching of the system was done every 250 steps. The optimized structures and Fe plane were used for the simulation. The representative snapshots of the sulphonamide compounds are shown in Figure 10. The relationship quantified the adsorption energy from our calculation;

$$E_{\text{ads}} = E_{\text{tot}} - (E_{\text{inh}} + E_{\text{Fe}}) \quad (13)$$

Where E_{tot} represent the total energy of the adsorbed Molecule/metal couple in the gaseous phase, and E_{inh} and E_{Fe} show the strengths of the inhibitor and metal slab, respectively. A negative value of the adsorption energy shows a stable adsorption structure. The adsorption energies shown for A and B correspond to the average of five most stable representative adsorption arrangements of each molecule. The sizes of the adsorption energies obtained from our calculations -124.27 kcal/mol and -133.17 kcal/mol are all negative and of reasonable sizes indicating stable structure. The pattern in the adsorption energy is related to the size of the molecular showing that the larger molecule adsorbed more firmly on the surface of the metal. This strong attraction to the metal surface accounts for the high inhibiting tendencies observed in the experimental result. The theoretical results agree well with our experimental results showing that compound B may be a better inhibitor than compound A this may be attributed to its larger molecular size.

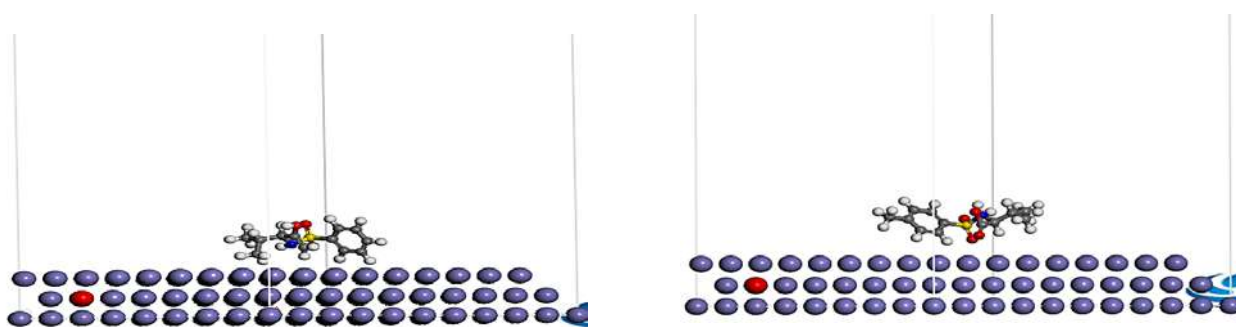


Figure 10 Representative snapshots of the sulphonamide compounds

4. Conclusion

The experimental and theoretical results have shown that the chosen sulphonamide compounds reduced the corrosion of the metal in 1 M KOH solution as well as retarded the microbial growth of *Proteus mirabilis* MW016889, *Enterobacter hormaechei* MW016890, *Bacillus* sp MW016891 and *Thiobacillus* sp. The

gravimetric results indicated that the corrosion retardation effect of the compounds increased with concentration increase; the electrochemical results show that the inhibition was due to the surface assimilation of the sulphonamide compounds on the metal surface. High values of inhibition efficiencies were observed both in the gravimetric and electrochemical experiments. Density functional theory rooted in Quantum chemical computation and molecule dynamic simulations further confirmed the inhibition properties of the compounds. The sulphonamide compounds also showed microbial growth inhibition against *Proteus mirabilis* MW01 6889, *Enterobacter hormaechei* MW016890, *Bacillus* sp MW016891 and *Thiobacillus* sp with the inhibition being more pronounced against *Proteus mirabilis* MW016 889 and *Bacillus* sp MW016891 for compound A. For compound B, inhibitory activity was more effective against *Thiobacillus* sp and *Enterobacter hormaechei* MW016890

Data availability

Bacteria Sequence data generated from this study have been deposited to GenBank under accession MW016889- MW016891.

5. References

1. El-Meligi, A A. Corrosion Preventive Strategies as a Crucial Need for Decreasing Environmental Pollution and Saving Economics, Recent Patents on Corrosion Science. 2010; 2: 22-33.
2. Marzorati S, Verotta L, Trasatti S P. Green Corrosion Inhibitors from Natural Sources and Biomass Wastes. Molecules (Basel, Switzerland). 2018; 48: 1-24 **DOI:** 10.3390/molecules24010048.
3. Muhammad A Q, Mahmood A, Muhammad I. Synthesis, Characterization, and Antibacterial Activities of Novel Sulfonamides Derived through Condensation of Amino Group Containing Drugs, Amino Acids, and Their Analogs", BioMed Research Inter., **2015**; 2015: 1-7 ([DOI:10.1155/2015/938486](https://doi.org/10.1155/2015/938486)).
4. Muhammad A Q, Mahmood A, Hina A, Sadia W, Muhammad I S. Amidine Sulfonamides and Benzene Sulfonamides: Synthesis and Their Biological Evaluation, J. Chem, 2015; 2015:1- 8 [DOI:10.1155/2015/524056](https://doi.org/10.1155/2015/524056).
5. Igwe C N, Okoro U O. Synthesis, Characterization, and Evaluation for Antibacterial and Antifungal Activities of N-Heteroaryl Substituted Benzene Sulphonamides, Org. Chem. Int. 2014; 2014: 1-5, **DOI:**10.1155/2014/419518.
6. Nardy K, Johannes A V, The dual role of microbes in corrosion, ISME J. 2015; 9: 542–551 **DOI:**10.1038/ismej.2014.169.

7. Oguzie E E, Ogukwe C E, Ogbulie J N, Nwanebu F C, Adindu C B, Udeze I. O K, Oguzie L, Eze F C. Broad spectrum corrosion inhibition: corrosion and microbial (SRB) growth inhibiting effects of Piper guineense extract, *J. Mater. Sci.* 2012; 47: 3592–3601, **DOI:** [10.1007/s10853-011-6205-1](https://doi.org/10.1007/s10853-011-6205-1).
8. Oguzie E E, Oguzie K L, Akalezi C O, Udeze I O, Ogbulie J N, Njoku V O. Natural Products for Materials Protection: Corrosion and Microbial Growth Inhibition Using Capsicum frutescens Biomass Extracts, *ACS Sustainable Chem. Eng.* 2013; 1: 214–225, **DOI:** [org/10.1021/sc300145k](https://doi.org/10.1021/sc300145k).
9. Hadi J S, Bhkakh C K, Corrosion, inhibition and biological evaluation investigations of Schiff bases derived from formyl chromone, *Adv Appl Sci Res.* 2015; 6: 103-112
10. Lalekan T P. Progress on pharmaceutical drugs, plant extracts and ionic liquids as corrosion inhibitors, *Heliyon* 2019; 5: 1-60 **DOI:** [10.1016/j.heliyon.2019.e01143](https://doi.org/10.1016/j.heliyon.2019.e01143).
11. Ikpa C B C, Okoro U C, Ubochi C I, Nwanorh K O. Synthesis, Characterization and Antibacterial Activity of 2-Phenylsulphonamide Derivatives of Some Amino Acids, *Inter. Letters of Chem. Phy. and Astronomy* 2016; 70: 42-47
12. Ikpa C B C, Okoro UC. Synthesis of New Paratoluene Sulphonamide Derivatives of Amino Acids and Their Anti-Bacterial Activities, *IOSR J. Applied Chem. (IOSR-JAC)* 2016; 9: 31-34
13. Ajeigbe S O, Basar N, Hassan M A, Aziz M. Optimization of Corrosion Inhibition of Essential oils of Alpinia galanga on mild steel using response surface methodology, *ARPN J of Eng. and Applied Sci.* 2017; 12: 2763-2771
14. Umoren SA, Obot I B, Gasem Z M. Adsorption and corrosion inhibition characteristics of strawberry fruit extract at steel/acids interfaces: experimental and theoretical approaches. *Ionics* 2015; 21: 1171–1186 **DOI:** [10.1007/s11581-014-1280-3](https://doi.org/10.1007/s11581-014-1280-3).
15. Ngobiri N C, Oguzie E E, Li Y, Liu L, Oforka N C, Akaranta IO. Eco-Friendly Corrosion Inhibition of Pipeline Steel Using Brassica oleracea, *Hindawi Publishing Corp. Intern. Journal Corr.* 2015; 2015: 1-9 **DOI:** [10.1155/2015/404139](https://doi.org/10.1155/2015/404139).
16. Adindu B, Ogukwe C, Eze F, Oguzie E. Exploiting the Anticorrosion Effects of Vernonia Amygdalina Extract for Protection of Mild Steel in Acidic Environments, *J. Electrochem. Sci. Technol.* 2016; 4: 251-262
17. Adindu B C Oguzie E E. Investigating the extract constituents and corrosion inhibiting ability of Sida acuta leaves, *World news of natural sciences* 2017; 13: 63-81
18. Mount D W. Using the basic local alignment search tool (BLAST) 2007; 14: **DOI:** [10.1101/pdb.top17](https://doi.org/10.1101/pdb.top17).

19. James A O, Oforka N C, Abiola O K, Ita B I. A study on the inhibition of mild steel corrosion in hydrochloric acid by pyridoxol hydrochloride, *Ecl. Quím., São Paulo* 2007; 32: 31-38 [DOI:10.1590/S0100-46702007000300005](https://doi.org/10.1590/S0100-46702007000300005).
20. Njoku VO, Oguzie E E, Obi C, Ayuk A A. "Baphia nitida Leaves Extract as a Green Corrosion Inhibitor for the Corrosion of Mild Steel in Acidic Media", *Advances in Chemistry*, **2014; 2014**: 1-10 [DOI: 10.1155/2014/808456](https://doi.org/10.1155/2014/808456).
21. Umoren S, Obot I B, Gasem Z, Odewunmi N A. Experimental and Theoretical Studies of Red Apple Fruit Extract as Green Corrosion Inhibitor for Mild Steel in HCl Solution, *J. Dispersion Sci. and Tech.* 2015; 36: 789-802 [DOI; 10.1080/01932691.2014.922887](https://doi.org/10.1080/01932691.2014.922887).
22. Ameh P O, Eddy N O. Theoretical and experimental studies on the corrosion inhibition potentials of 3-nitrobenzoic acid for mild steel in 0.1 M H₂S₄, *Cogent Chemistry* 2016; 2: 1-18, (2016) [DOI: 10.1080/23312009.2016.1253904](https://doi.org/10.1080/23312009.2016.1253904).
23. Abdel-Rehim S S, Khaled KF, Al-Mobarak N A. Corrosion inhibition of iron in hydrochloric acid using pyrazole, *Arab. J. Chem.* 2011; 4: 333–337 ([DOI: 10.1016/j.arabjc.2010.06.056](https://doi.org/10.1016/j.arabjc.2010.06.056)).
24. Momoh-Yahaya H, Eddy N O, Oguzie E E. Inhibitive, Adsorptive and Thermodynamic Study of Hypoxanthine against the Corrosion of Aluminium and Mild Steel in Sulphuric Acid, *J. Mater. Environ. Sci.* 2014; 5: 237-244
25. Ogukwe C E, Akalezi C O, Chidiebere M A, Oguzie K L, Iheabunike Z O, Oguzie E E. Corrosion Inhibition and Adsorption of Anthocleista Djalonesis Leaf Extract on the Acid Corrosion of Mild Steel, *Port. Electrochim. Acta*, 2012; 30: 189-202 [DOI:10.4152/pea.201203189](https://doi.org/10.4152/pea.201203189).
26. NCCLS. Performance Standards for Antimicrobial Disc Susceptibility Tests. Approved Standard NCCLS Publication M2-A5, Villanova, PA, USA (1993)
- 27 Khan M, Saha M, Begum N, Islam M, Hoque S. Isolation and characterization of bacteria from rusted iron materials. *Bangl. J. Bot.* 2010; 39: 185-191 [DOI: 10.3329/bjb.v39i2.7479](https://doi.org/10.3329/bjb.v39i2.7479).
28. Okabe S, Odagiri M, Ito T Satoh H. Succession of Sulfur-Oxidizing Bacteria in the Microbial Community on Corroding Concrete in Sewer Systems. *Appl. Environ. Microbiol.* **2017**; 73: 971-980 [DOI: 10.1128/AEM.02054-06](https://doi.org/10.1128/AEM.02054-06).

29. Huber B, Herzog B, Drewes J E, Koch K, Muller E. Characterization of sulfur oxidizing bacteria related to biogenic sulfuric acid corrosion in sludge digesters. *BMC Microbiol* 2016; 16: 1-11 [DOI:10.1186/s12866-016-0767-7](https://doi.org/10.1186/s12866-016-0767-7).
30. Singh A, Caihong Y, Yaocheng Y, Soni N, Wu Y, Lin Y. Analyses of New Electrochemical Techniques to Study the Behavior of Some Corrosion Mitigating Polymers on N80 Tubing Steel. *ACS omega*, 2019; 4: 3420-3431 [DOI:10.1021/acsomega.8b02983](https://doi.org/10.1021/acsomega.8b02983).
31. Akalezi C O, Enenebaku C K, Oguzie E E. Application of aqueous extracts of coffee senna for control of mild steel corrosion in acidic environments. *Int. J. Ind. Chem.* 2012; 3: 1-12 [DOI: 10.1186/2228-5547-3-13](https://doi.org/10.1186/2228-5547-3-13).
- 32 Eddy N O, Momoh-Yahaya H, Oguzie E E. Theoretical and experimental studies on the corrosion inhibition potentials of some purines for aluminum in 0.1 M HCl, *J. Advanced Research* 2015; 6: 203-217 (2015) [DOI:10.1016/j.jare.2014.01](https://doi.org/10.1016/j.jare.2014.01).
33. Oguike R S, Oni O. Computational Simulation and Inhibitive Properties of Amino acids for Mild Steel Corrosion: Adsorption in Gas Phase onto Fe (110), *International Journal of Research in Chemistry and Environment*, *Int. J. Res. Chem. Environ.*, 2014; 4: 177-186 [DOI: 10.1155/2013/175910](https://doi.org/10.1155/2013/175910).
34. Oguike R S, Omizegba F, Oni O, Akanang H, Shibdawa A M. Adsorption Behaviour of Vitex doniana on Annealed Carbon Steel Corrosion in Hydrochloric Acid: Experimental and Theoretical investigations, *Der Pharma Chemica*, 2017; 9: 79-91.
35. Usman B, Jimoh I, Umar B A. Theoretical study of 2 - (3, 4-dihydroxyphenyl) chroman-3, 5, 7-triol on corrosion inhibition of mild steel in acidic medium, *Appl. J. Envir. Eng. Sci.* 2019; 5: 66-74
36. Casewit C J, Colwell K S, Rappé A K. Application of a universal force field to organic molecules *Journal of the American Chemical Society*, *J. Am. Chem. Soc*, 1992a; 114: 10035–10046.
37. Casewit C J Colwell K S, Rappé A K. Application of a universal force field to main group compounds *Journal of the, J. Am. Chem. Soc*, 1992b; 114: 10046–10053 .
38. Oguzie E E, Li Y, Wang S G, Wang F. Understanding corrosion inhibition mechanisms experimental and theoretical approach, *RSC Adv.*, 1, 866-873, [DOI:10.1039/C1RA00148E](https://doi.org/10.1039/C1RA00148E).
39. Awe F E, Idris S O, Abdulwahab M, Oguzie E E. Theoretical and experimental inhibitive properties of mild steel in HCl by ethanolic extract of *Boscia senegalensis*, *Cogent Chemistry*, 2015; 1: 1-14 [DOI: 10.1080/23312009.2015.1112676](https://doi.org/10.1080/23312009.2015.1112676).

40. Arukalam I O, Madufor I C, Ogbobe O, Oguzie E E. Acidic Corrosion Inhibition of Copper by Hydroxyethyl Cellulose, British Journal of Applied Science & Technology, 2014; 4: 9, 1445-1460 **DOI:** [10.9734/BJAST/2014/5463](https://doi.org/10.9734/BJAST/2014/5463).

© GSJ